

Preparation and Properties of Poly(propylene carbonate) and Nanosized ZnO Composite Films for Packaging Applications

Jongchul Seo,¹ Gwonyoung Jeon,¹ EUi Sung Jang,² Sher Bahadar Khan,^{2,3} Haksoo Han²

¹Department of Packaging, Yonsei University, 234 Maeji-ri, Heungup-myun, Wonju-si, Kangwon-do 220-710, Korea

²Department of Chemical and Biomolecular Engineering, Yonsei University, 262 Seongsanno, Seodaemun-gu, Seoul 120-749, Korea

³Centre for Advanced Materials and Nano-Engineering (CAMNE) and Department of Chemistry, Faculty of Sciences and Arts, Najran University, P. O. Box 1988, Najran, 11001, Kingdom of Saudi Arabia

Received 6 July 2010; accepted 25 January 2011

DOI 10.1002/app.34248

Published online 20 May 2011 in Wiley Online Library (wileyonlinelibrary.com).

ABSTRACT: A series of polypropylene carbonate (PPC)/ZnO nanocomposite films with different ZnO contents were prepared via a solution blending method. The morphological structures, thermal properties, oxygen permeability, water sorption, and antibacterial properties of the films were investigated as a function of ZnO concentration. While all of the composite films with less than 5 wt % ZnO exhibited good dispersion of ZnO in the PPC matrix, FTIR and SEM results revealed that solution blending did not lead to a strong interaction between PPC and unmodified ZnO. As such, poor dispersion was induced in the composite films with a high ZnO content. By incorporating inorganic ZnO filler nanoparticles, the diffusion coefficient, water uptake in equilibrium, and oxygen permeability decreased as the content of ZnO increased. The PPC/ZnO nanocomposite films also displayed a good inhibitory effect

on the growth of bacteria in the antimicrobial analysis. The enhancement in the physical properties achieved by incorporating ZnO is advantageous in packaging applications, where antimicrobial and environmental-friendly properties, as well as good water and oxygen barrier characteristics are required. Furthermore, UV light below ~ 350 nm can be efficiently absorbed by incorporating ZnO nanoparticles into a PPC matrix. ZnO nanoparticles can also improve the weatherability of a PPC film. In future research, the compatibility and dispersion of the PPC matrix polymer and the inorganic ZnO filler nanoparticles should be increased. © 2011 Wiley Periodicals, Inc. *J Appl Polym Sci* 122: 1101–1108, 2011

Key words: polypropylene carbonate; ZnO nanoparticles; water sorption; antibacterial property; packaging materials; morphological structure

INTRODUCTION

The utilization of carbon dioxide has attracted scientific and practical interest in recent years because of environmental pollution and energy shortages.^{1–3} Global warming, also known as the greenhouse effect, is primarily caused by the massive release of carbon dioxide into the atmosphere. The contribution of carbon dioxide to global warming is estimated to be about 66%. Thus, the incorporation of carbon dioxide into materials has attracted a great deal of interest as a means to reduce greenhouse gas pollution and is

viewed as an alternative to overcome shortages in conventional petroleum fuel supplies.

Among the polymeric materials that use carbon dioxide, polypropylene carbonate (PPC) was first synthesized by Inoue and Tsuruta via the copolymerization of carbon dioxide and propylene oxide.⁴ PPC is a biodegradable aliphatic polycarbonate that can be degraded to H₂O and carbon dioxide. The synthesis of PPC allows for carbon dioxide to be recycled in the environment. PPC has interesting chemical and physical properties, such as compatibility, impact resistance, translucence, and innocuousness. Such properties are advantageous in adhesives, solid electrolytes, barrier materials, plasticizers, and new materials for packaging applications. Much research has been devoted to improve the thermal and mechanical properties of PPC by blending it with other polymers^{5–7} or inorganic fillers.^{8–11}

Because of the nanoscale sizes and large specific surface areas of nanosized fillers, the interfacial interaction between the filler and the polymer is strong, resulting in a large improvement in the

Correspondence to: H. Han (hshan@yonsei.ac.kr).

Contract grant sponsor: National Research Foundation of Korea (MEST); contract grant number: (NRF-2009-C1AAA001-0092926).

Contract grant sponsor: New and Renewable Energy R and D Program, Ministry of Knowledge Economy, Republic of Korea; contract grant number: 2009T100100606.

physical properties of the polymer. Xu et al.⁹ and Shi and Gan¹¹ prepared intercalated-exfoliated PPC/montmorillonite nanocomposites by direct melt blending in an internal mixer and by solution intercalation, respectively. The thermal decomposition temperature and storage modulus of the structures with even a low concentration of montmorillonite were much higher than those attained with PPC. Li et al.⁸ showed that composites of PPC reinforced with microscale and nanoscale calcium carbonate particles exhibited a decrease in tensile strength because of the agglomeration of calcium carbonate nanoparticles during blending. However, nanosized zinc oxide (ZnO), as a functional inorganic filler, has been widely used in functional devices, catalysts, pigments, optical materials, cosmetics, UV-absorbers, and additives in many industrial products.^{12–17} Recently, there have been several published reports regarding the antimicrobial activity of ZnO nanoparticles.^{12,13,18}

To the best of our knowledge, there have been no reports on PPC/ZnO nanocomposite films and their properties for use as packaging materials. In this article, five different PPC/ZnO nanocomposite films were prepared via solution blending, and the effects of the ZnO content on the morphological structure, thermal properties, oxygen permeability, water sorption, and antibacterial properties of the films were investigated.

EXPERIMENTAL

Materials

PPC resin with a number-average molecular weight (M_n) of 240,000 g/mol was provided by SK Energy Co. (Chunan, Korea). Inorganic ZnO nanoparticles with an average size of 40 nm were supplied by Sukgyung AT Co. (Ansan, Korea). Acetone was purchased from Aldrich Chemical Co. (Yongin, Korea) and used as-received.

Preparation of PPC/ZnO nanocomposite films

Five different compositions of PPC/ZnO nanocomposite films with PPC/ZnO weight ratios of 100/0, 99/1, 97/3, 95/5, and 90/10 were prepared by the solution blending method.¹⁶ A solution containing the proper amount of ZnO was first dispersed in acetone, sonicated for 30 min, and mechanically stirred for another 10 min. PPC was then added to the solution and continuous stirring was performed for 3 h at room temperature. The mixed solution was cast onto a glass plate and dried in a drying oven at 60°C for 10 h so as to remove any solvent. After the solvent was completely removed, the composite films were extracted from the oven, dipped in deion-

ized water, and then stored in a desiccator at room temperature for further study.

Measurements

The Fourier transform infrared (FTIR) spectra of the PPC/ZnO nanocomposite films were collected with an Excalibur Series FT-IR (Digilab, Model Varian 4100, MA) instrument in transmission mode; the wavenumber range was set from 4000 to 400 cm^{-1} . The UV-visible spectra of the PPC/ZnO nanocomposite films were recorded with a single-beam UV spectrometer (Mecasys, Model OPTIZEN 2120UV, Daejeon, Korea) in the range of 200–800 nm, and a blank glass plate was employed as a reference.

The thermal decomposition profiles of the PPC/ZnO nanocomposite films were thermogravimetrically analyzed with a TA Instruments Q50 TGA (DE). Film samples ranging from 4 to 6 mg were placed on a platinum pan and heated from 30 to 500°C in an N_2 atmosphere at a heating rate of 10°C/min. The weight loss in the samples was then recorded as a function of temperature.

To analyze the morphology of the PPC/ZnO nanocomposite films, wide-angle X-ray diffraction (WAXD) patterns were obtained using a wide-angle goniometer (Rigaku, Model RINT 2500H, Tokyo, Japan) with a monochromator (flat crystal type). The $\text{Cu K}\alpha$ ($\alpha = 1.54 \text{ \AA}$) radiation source was operated at 40 kV and 40 mA; all measurements were carried out in $\theta/2\theta$ mode. Data were collected in the range of 5–60° at 0.02° intervals with a scan speed of 1.0°/min. To investigate the dispersion of ZnO nanoparticles in the PPC matrix, the fractured surfaces of the PPC/ZnO nanocomposite films were observed with a scanning electron microscope (SEM, Hitachi, Model S-4200, Tokyo, Japan). For the fractured surface measurements, the films were frozen in liquid nitrogen and broken to produce a cross section. Prior to the examination, the samples were coated with a thin layer of gold. The morphology of the PPC/ZnO nanocomposite films was also examined via transmission electron microscopy (TEM) with a Hitachi electron microscope. The samples for the TEM analysis were sectioned with an ultramicrotome.

The water sorption behaviors of the PPC/ZnO nanocomposite films were gravimetrically investigated with a thin film diffusion analyzer (Cahn Instruments, Model D-200, CA).^{19–21} The water sorption isotherms were measured at 25°C and 100% relative humidity. The details of the isotherm measurement procedure are described in our previous studies.^{20,21} The oxygen transmission rates (OTRs) of the PPC/ZnO nanocomposite films were measured with an oxygen permeation analyzer (Illinois Instruments Inc., Model 8001, IL) following ASTM Standard D 3985.

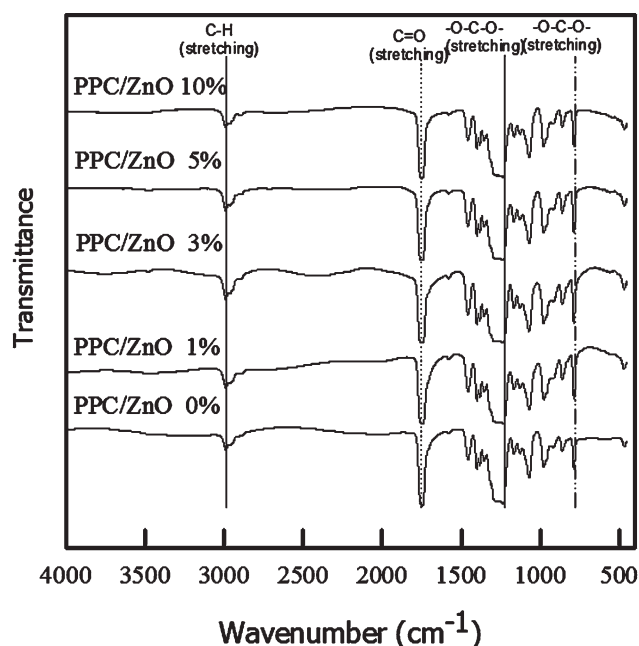


Figure 1 FTIR spectra of a pure PPC film and the PPC/ZnO nanocomposite films.

Antibacterial tests of the PPC/ZnO nanocomposite films were carried out according to the JIS Z 2801 standard²²; *E. coli* and *Lactobacillus* were employed as the target organisms for the Gram-negative and Gram-positive bacteria, respectively. The bacteria were individually grown on Luria-Bertani (LB) agar plates at 30°C for 24 h and resuspended in sterile physiological saline (PS) to an optical density of 1.2 at 600 nm. The prepared composite films were then placed on a sterile plate, and the suspension (20 μ L) was dropped on the films. These carrier films were maintained at temperatures below $37 \pm 1^\circ\text{C}$ and at a relative humidity $>90\%$. After 24 h, the bacteria were washed off with PS, and 100 μ L of a serial dilution of the suspension was plated onto the LB agar. The colony forming units (CFUs) of the bacteria were counted, and the antibacterial rate (R) was calculated via the following equation:

$$\%R = [(B - C)/B] \times 100\% \quad (1)$$

where B and C are the CFU of viable cells of the bacteria on the control sample and the PPC/ZnO composite samples after 24 h, respectively.

RESULTS AND DISCUSSION

Preparation of PPC/ZnO nanocomposite films

Interfacial interactions between polymer and inorganic components in composites can be identified through an analysis of FTIR spectra. If a good chemical interaction between the polymer matrix and the

inorganic exists, an appreciable change in the FTIR spectra of the composite films are observed by adding each component.^{16,17} The FTIR spectra of a pure PPC film and four different PPC/ZnO nanocomposite films are shown in Figure 1. In the FTIR spectrum of pure PPC, a characteristic vibration band of C=O stretching is observed at 1750 cm^{-1} , those of C—O stretching are found at 1223 and 775 cm^{-1} , and that of C—H stretching is observed at 2985 cm^{-1} . The spectra of the PPC/ZnO nanocomposite films clearly exhibit characteristic absorption peaks corresponding to only polymeric groups of pure PPC. That is, the FTIR spectra of the nanocomposite films show no apparent change or shift in the characteristic peaks of pure PPC with the addition of ZnO particles. The pure PPC and PPC/ZnO nanocomposite films yielded the same FTIR spectra, which means a poor chemical interaction between the PPC and ZnO occurred, or the ZnO characteristic peak was overlapped by the PPC characteristic peak. ZnO nanoparticles are generally polar, and thus, strong self-interaction is induced between the nanoparticles. Such a scenario results in hard agglomerates.^{13,23} The high polarity of ZnO nanoparticles impedes the chemical interaction between ZnO and the PPC matrix. This in turn causes no change or shift in the characteristic peak found in the FTIR analysis. Further research is needed to improve the chemical interaction between the PPC and ZnO by modifying the surface of the ZnO, as described in previous studies.^{12,14–17}

Optical properties

The optical properties of the PPC/ZnO nanocomposite films were measured with a UV spectrometer; the results are presented in Figure 2. In the absorption curves of the PPC/ZnO nanocomposite films, an absorption peak appeared at 200–370 nm in all of the samples containing ZnO nanoparticles. The UV absorption of the PPC/ZnO nanocomposite films was much higher than that of the pure PPC film. In addition, the UV absorption intensity in the region of the flanks increased with increasing ZnO nanoparticle content. As such, UV light below $\sim 350\text{ nm}$ can be efficiently absorbed by incorporating ZnO nanoparticles into a PPC matrix. ZnO nanoparticles can thus improve the weatherability of a PPC film, and the composite structure can potentially be applied to UV-protecting and optical materials such as coatings, cosmetics, and plastics.^{14,16}

Thermal properties

The thermal degradation curves for a pure PPC film and four PPC/ZnO nanocomposite films with different compositions are shown in Figure 3. Regardless

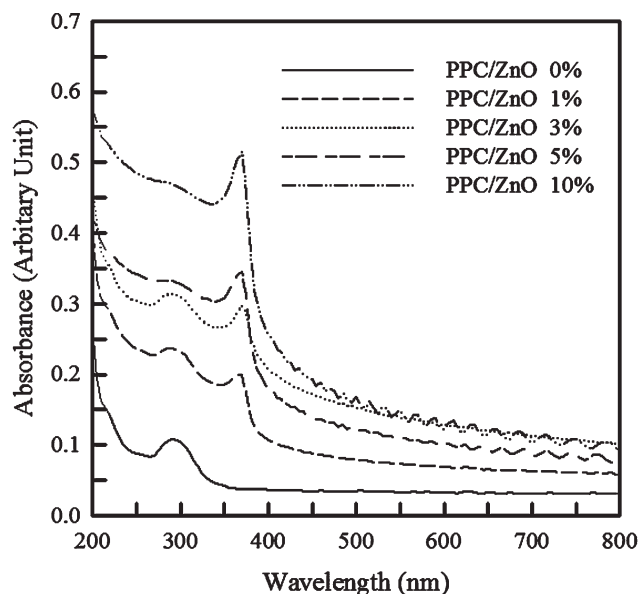


Figure 2 UV absorption spectra of the PPC/ZnO nano-composite films.

of the amount of ZnO, all of the PPC/ZnO nano-composite films exhibit a steep decrease in weight in the range of 240–300°C. Such a trend was also observed with a pure PPC film. The TGA and derivative thermogravimetry (DTG) curves reveal that PPC decomposes in two steps [see Fig. 3(b)] when no ZnO is present, which is consistent with the results of previous studies.² The thermal degradation of PPC generally occurs by random main chain scission and then unzipping.^{1–3} In contrast, the thermal decomposition of PPC/ZnO composites occurs in one step. Therefore, it can be deduced that the introduction of ZnO into a PPC matrix may change the mechanism of thermal degradation in PPC. In addition, bare ZnO nanoparticles have a higher thermal stability than the polymer matrix; so it is anticipated that the incorporation of ZnO particles will improve the thermal stability of pure PPC. However, the thermal stability of the composite films was found to decrease with an increase in the ZnO content, as shown in Figure 3(a). Such a result may be due to the inherent nature of ZnO and/or the existence of morphological imperfections as the content of ZnO is increased.

From the results of a pyrolysis gas chromatographic analysis, Inoue and Tsuruta⁴ suggested that the thermal degradation of PPC occurs in two steps: a scission reaction of the backbone, followed by an unzipping reaction. Carbon dioxide and propylene oxide are ultimately produced. According to the literature,^{2,24} catalysts do not affect the decomposition mechanism but slightly reduce the activation energy and accelerate the depolymerization reaction. Among the catalysts employed in previous studies, catalyst precursors containing zinc or other metals

have been found to improve the catalytic efficiency and copolymerization processes. Therefore, it is anticipated that the incorporation of zinc oxide into a PPC matrix may affect the degradation of PPC by reducing the activation energy and increasing the scission reaction rate of the backbone. As demonstrated with the FTIR results presented earlier, a strong interfacial interaction does not exist between the PPC and ZnO nanoparticles. Therefore, an increase in the thermal stability of the PPC may not occur. However, further insight into the increased degradation of PPC by the incorporation of ZnO is needed.

Morphological structure

The morphological structure of organic/inorganic composites is a very important characteristic, because it ultimately affects the thermal stability, mechanical properties, and water and gas permeability of the structures. The effects of ZnO nanoparticles on the morphological structure of the PPC/ZnO nanocomposite films were investigated via WAXD and SEM.

The WAXD patterns of the PPC/ZnO nanocomposite films are shown in Figure 4. A broad noncrystalline peak of PPC is observed in the range of 10–30°, and several sharp diffraction peaks of ZnO are also present. The incorporation of ZnO nanoparticles did not produce new peaks with respect to pure PPC, indicating that ZnO-filled PPC nanocomposites consist of two phase structures: polymer and nanoparticles. As the ZnO content was increased from 0 to 10 wt %, the 2θ value of the peak increased from 19.1° to 19.8°. The Bragg equation was used to

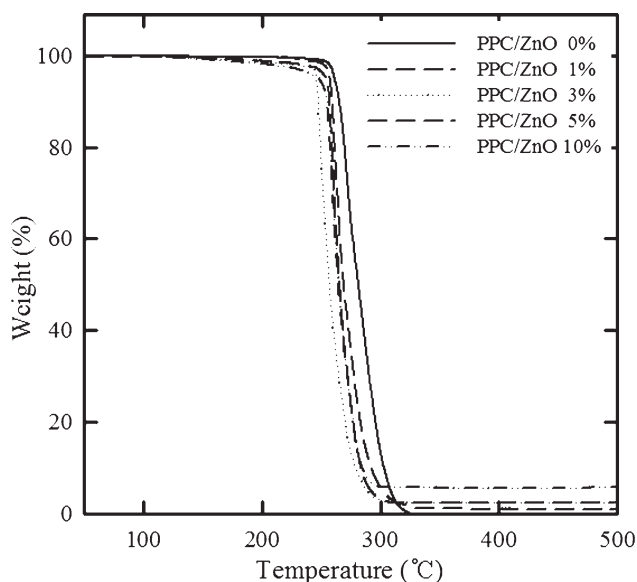


Figure 3 TGA/DTG thermograms of the PPC/ZnO nano-composite films.

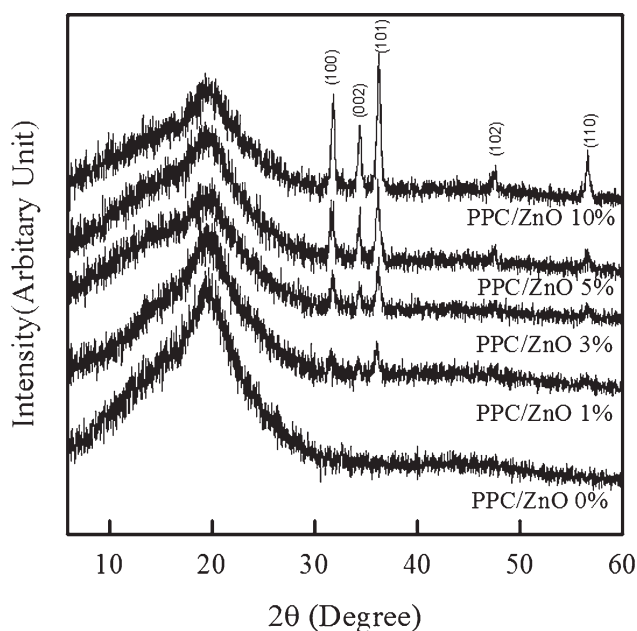


Figure 4 WAXD patterns of the PPC/ZnO nanocomposite films.

calculate the mean intermolecular distance; the distance decreased from 4.71 to 4.54 Å as the ZnO content was increased. While the incorporation of ZnO did not have a significant effect on the morphological structure of the PPC, the WAXD results indicate that the introduction of ZnO enhanced molecular ordering in the amorphous and structureless polymer. Such a scenario may induce a decrease in the water diffusion and gas barrier properties in pure PPC films.

Shown in Figure 5(a–e) are SEM images of the fractured surfaces of the PPC/ZnO nanocomposite films, respectively. The white spots in the images indicate ZnO nanoparticles. When the ZnO content was less than 5%, no aggregation of the ZnO particles in the PPC matrices was observed in both the surface and fractured surface micrographs. As such, ZnO nanoparticles were well-dispersed in the matrices of the composite films with a ZnO content of less than 5%. In contrast, agglomeration of ZnO was apparent in both the top surface and the fractured surface for the composite films containing 10% ZnO nanoparticles. This can be confirmed by the TEM investigations as shown in Figure 6. Whereas no large ZnO agglomerations were observed in 3% PPC/ZnO nanocomposite films, the composite film with 10% ZnO showed apparent agglomeration of ZnO in the PPC matrix. This inhomogeneous dispersion of fillers and imperfect morphology can yield adverse effects on the thermal properties, water sorption, and gas permeabilities of the PPC/ZnO nanocomposite films. In general, the formation of Zn–O–Zn bonds among the nanoparticles due to the existence of water molecules results in hard agglomerates, which impede the applicability of the ZnO nanoparticles.²³

Water sorption and oxygen permeability

In packaging applications, a higher moisture content and fast moisture/gas transmission considerably restrict its use as potential packaging materials.

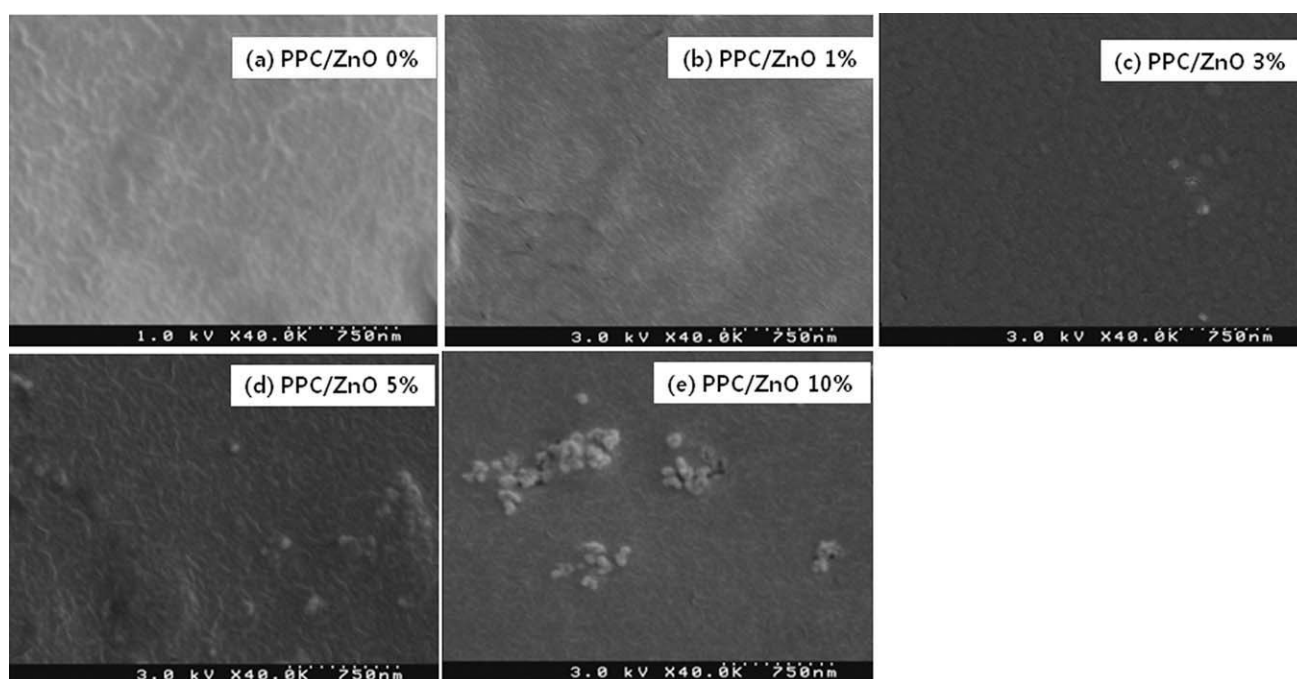


Figure 5 SEM images of the fractured surfaces of the PPC/ZnO nanocomposite films.

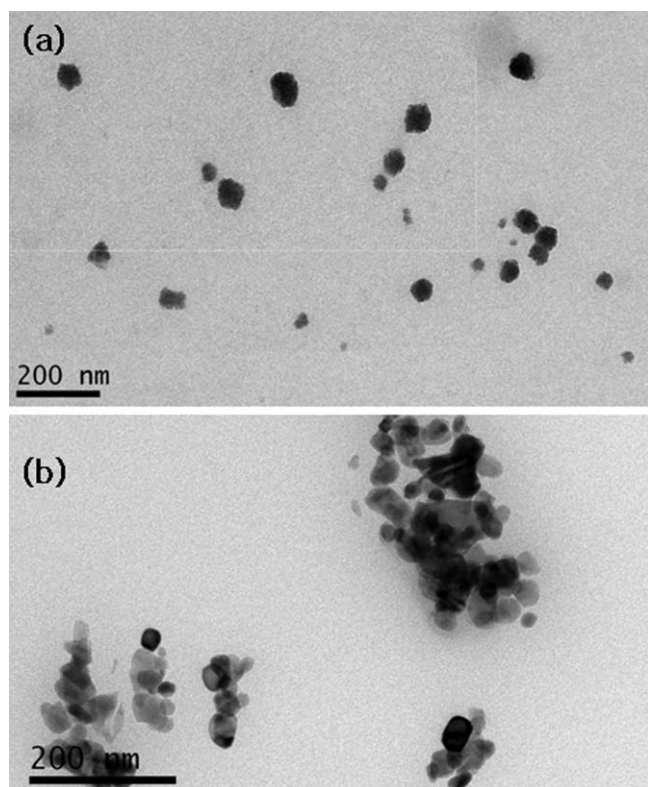


Figure 6 TEM patterns of the PPC/ZnO nanocomposite films: (a) ZnO 3% and (b) ZnO 10%.

Thus, the water sorption behaviors of the PPC/ZnO nanocomposite films were gravimetrically investigated at 25°C and 100% relative humidity^{20,21}; the results are shown in Figure 7. The water sorption isotherms are nearly Fickian, as is observed for vari-

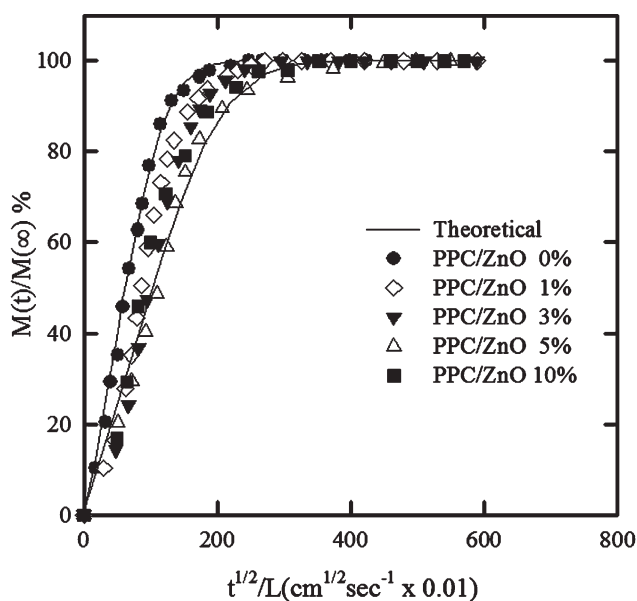


Figure 7 Water sorption isotherms of the PPC/ZnO nanocomposite films measured at 25°C and 100% relative humidity.

ous polymers in films.¹⁹ Therefore, all of the measured sorption isotherms were analyzed with the following equation, which is the mathematical solution for water diffusion in an infinite slab with a constant surface concentration^{19–21}:

$$\frac{M(t)}{M(\infty)} = 1 - \frac{8}{\pi^2} \sum_{m=0}^{\infty} \frac{1}{(2m+1)^2} \exp\left(\frac{-D(2m+1)^2 \pi^2 t}{L^2}\right) \quad (2)$$

where $M(t)$ is the water uptake at time t , $M(\infty)$ is the water uptake at $t = \infty$, D (cm^2/sec) is the diffusion coefficient of water, and L is the thickness of the PPC/ZnO composite film. The experimental data for the entire range were fitted with Eq. (2), leading to an estimation of the diffusion coefficient and water uptake. The results are summarized in Table I.

The pure PPC film yielded a diffusion coefficient of $12.0 \times 10^{-10} \text{ cm}^2/\text{sec}$ and a water uptake of 2.01 wt %; the composite films with ZnO exhibited a relatively lower diffusion coefficient and water uptake. Both the diffusion coefficient and the water uptake decreased as the content of ZnO in the PPC was increased. This indicates that the water resistance capacity of PPC is greatly enhanced with the incorporation of ZnO. However, when compared with the PPC/ZnO composite film with 5% ZnO, the 10% ZnO sample did not exhibit a noticeable decrease in the diffusion coefficient and water uptake. Such a result may be due to imperfections in the morphology.^{20,21} The OTRs of the PPC/ZnO nanocomposite films were also investigated with an oxygen permeation analyzer. As shown in Table I, a neat PPC film exhibited an OTR of 554 $\text{mL}/\text{m}^2 \text{ day}$, while the samples with ZnO particles yielded relatively lower OTRs. As displayed in Figure 8, the OTR decreased as the content of ZnO in the PPC was increased. Such a trend was also observed in the diffusion coefficient and water uptake data obtained from the water sorption experiments.

The water sorption and oxygen permeability analyses revealed that the incorporation of ZnO particles leads to a reduction in the transmission rate and the amount of penetrant. Such findings indicate a decrease in both the potential capacity of the PPC matrix to sorb permeant molecules and the ability of those molecules to diffuse through the polymeric material. However, the composite film with 10% ZnO exhibited a relatively high diffusion coefficient, water uptake, and OTR.

In general, the diffusion and barrier performance of a polymer film is strongly dependent on the morphological structure of the films, which includes the crystallinity, orientation, chain stiffness, free volume, and cohesive energy density of the polymer. The addition of inorganic fillers typically increases the

TABLE I
Diffusion Coefficient, Water Uptake, and Oxygen Transmission Rate of the PPC/ZnO Nanocomposite Films

Sample	Thickness (μm)	Diffusion coefficient ($\times 10^{-10} \text{ cm}^2/\text{sec}$)	Water uptake (wt %)	Oxygen transmission rate ($\text{mL}/\text{m}^2 \text{ day}$)
PPC/ZnO 0%	18	12.0	2.01	554
PPC/ZnO 1%	18	8.3	1.34	272
PPC/ZnO 3%	20	6.7	0.94	296
PPC/ZnO 5%	19	5.1	0.62	145
PPC/ZnO 10%	22	6.4	0.65	140

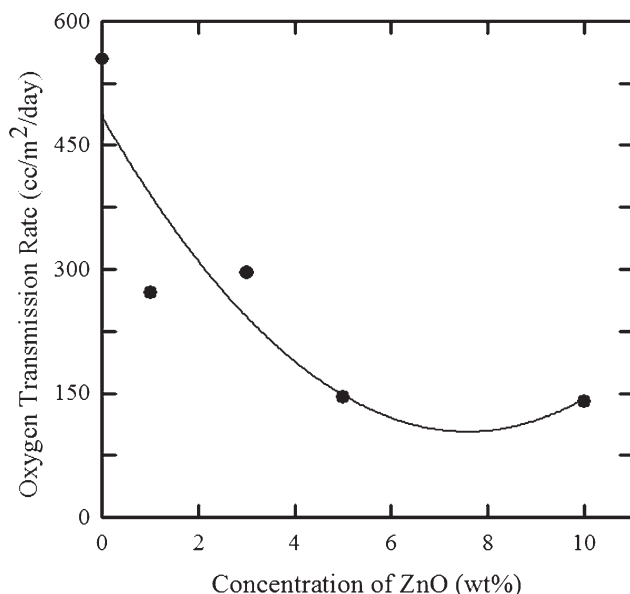


Figure 8 Oxygen transmission rate (OTR) of the PPC/ZnO nanocomposite films measured at 25°C.

barrier property of the penetrant if the inorganic filler has a high degree of adhesion and good compatibility with the matrix polymer. From analyses of the SEM images, the ZnO and the polymer in the composite film with 10% ZnO appeared to be incompatible and lacked adhesion. A poor interaction between the ZnO and PPC at the PPC/ZnO interface

and imperfections in morphology may lead to an increase in the free volume of the system and, consequently, less of a decrease in the water sorption and OTR of the 10% PPC/ZnO nanocomposite film.

Antibacterial properties

The antibacterial properties of plastics have attracted an increasing amount of attention.^{12,13,18,25,26} In this study, the antibacterial testing of the PPC/ZnO nanocomposite films was performed according to the JIS Z 2801 standard²²; *E. coli* and *Lactobacillus* were employed as the target organisms. The antibacterial test results and representative photographic images are given in Table II. Each sample was compared with a control sample that contained no ZnO.

As shown in Table II, the percentage reductions (%R value) for both *E. coli* and *Lactobacillus* are strongly dependent on the content of ZnO. The %R value for *E. coli* is 0.0% for the pure PPC film and 100% for the 10% ZnO composite film, while for *Lactobacillus*, the %R values are 0.0% and 87.5% for the pure PPC and 10% ZnO composite films, respectively. Such results indicate that a pure PPC film has no antibacterial activity against both *E. coli* and *Lactobacillus*. The antibacterial activity apparently increased with an increase in the content of ZnO.^{12,13,18} Furthermore, the PPC/ZnO nanocomposite films exhibited stronger inhibitory effects against *E. coli* than toward *Lactobacillus*. It can be concluded

TABLE II
Results of the Antibacterial Test of the PPC/ZnO Composite Films toward *E. coli* and *Lactobacillus*

		PPC/ZnO 0%	PPC/ZnO 1%	PPC/ZnO 3%	PPC/ZnO 5%	PPC/ZnO 10%
<i>E. coli</i>	Photo-image					
	%R ^a	0.0%	28.6%	66.7%	76.2%	100%
<i>Lactobacillus</i>	Photo-image					
	%R ^a	0.0%	22.5%	45.3%	60.2%	87.5%

^a % Reduction of viable bacterial cell ($= (B-C)/B \times 100\%$), where *B* and *C* are the average number of viable cells of bacteria on the control sample and the PPC/ZnO composite samples after 24 h, respectively.

that the antibacterial properties of the nanosized PPC/ZnO nanocomposite films are due to the ZnO nanoparticles. The antibacterial activity of ZnO is believed to be caused by the generation of hydrogen peroxide (H₂O₂) from the ZnO surface.¹⁸ As such, more ZnO in the polymer matrix should result in more antibacterial activity in polymer/ZnO composite films. In previous studies, the incorporation of ZnO into polymer films led to an inhibitory effect on the growth of Gram-negative bacteria such as *E. coli* and Gram-positive bacteria such as *Lactobacillus*.^{12,13,18}

CONCLUSIONS

Five PPC/ZnO nanocomposite films with different compositions were prepared, and their physical and antibacterial properties were investigated in terms of the ZnO content as required for packaging applications. While the PPC/ZnO nanocomposite films exhibited good dispersion in the range of 1–5 wt % ZnO, solution blending did not yield a strong interaction between the PPC and unmodified ZnO. By incorporating inorganic ZnO filler nanoparticles, the diffusion coefficient, water uptake, and oxygen permeability of the composite structures decreased as the content of ZnO was increased. In addition, the PPC/ZnO nanocomposite films displayed a good inhibitory effect on the growth of bacteria. The enhanced water/oxygen barrier properties and good antibacterial properties of PPC/ZnO nanocomposite films make them potential candidates for versatile packaging applications. However, further research is needed to increase the compatibility and dispersion of the PPC matrix polymer and inorganic ZnO filler nanoparticles.

References

1. Wang, S. J.; Du, L. C.; Zhao, X. S.; Tjong, S. C. *J Appl Polym Sci* 2002, 85, 2327.
2. Li, X. H.; Meng, Y. Z.; Zhu, Q.; Tjong, S. C. *Polym Degrad Stab* 2003, 81, 157.
3. Luinstra, G. A. *Polym Rev* 2008, 48, 192.
4. Inoue, S.; Tsuruta, T. *J Appl Polym Symp* 1975, 26, 257.
5. Ge, X. C.; Li, X. H.; Zhu, Q.; Li, L.; Meng, Y. Z. *Polym Eng Sci* 2004, 44, 2134.
6. Tao, J.; Song, C.; Cao, M.; Hu, D.; Liu, L.; Liu, N.; Wang, S. *Polym Degrad Stab* 2009, 94, 575.
7. Ma, X.; Yu, J.; Wang, N. *J Polym Sci Polym Phys* 2006, 44, 94.
8. Li, X. H.; Tjong, S.; Meng, Y. Z.; Zhu, Q. *J Polym Sci Polym Phys* 2003, 41, 1806.
9. Xu, J.; Li, R. K. R.; Meng, Y. Z.; Mai, Y. W. *Mater Res Bull* 2006, 41, 244.
10. Wan, C. J.; Yu, J. Y.; Shi, X. J.; Huang, L. H. *Trans Nonferrous Met Soc China* 2006, 16, 508.
11. Shi, X.; Gan, Z. *Macromol Nanotechnol* 2007, 43, 4852.
12. Li, J. H.; Hong, R. Y.; Li, M. Y.; Li, H. Z.; Zheng, Y.; Ding, J. *Progr Org Coat* 2009, 64, 504.
13. Chaurasia, V.; Chand, N.; Bajpai, S. K. *J Macromol Sci Pure Appl Chem* 2010, 47, 309.
14. Liu, P.; Su, Z. *J Macromol Sci Part B: Phy* 2006, 45, 131.
15. Hong, R. Y.; Chen, L. L.; Li, J. H.; Li, H. Z.; Zheng, Y.; Ding, J. *Polym Adv Technol* 2007, 18, 901.
16. Chae, D. W.; Kim, B. C. *Polym Adv Technol* 2005, 16, 846.
17. Tang, E.; Liu, H.; Sun, L.; Zheng, E.; Cheng, G. *Eur Polym Mater* 2007, 43, 4210.
18. Padmavathy, N.; Vijayaraghavan, R. *Sci Technol Adv Mat* 2008, 9, 1.
19. Crank, J.; Park, G. S. *Diffusion in Polymers*; Academic Press: London, 1968.
20. Seo, J.; Lee, C.; Jang, W.; Sundar, S.; Han, H. *J Appl Polym Sci* 2006, 99, 1692.
21. Seo, J.; Han, C. S.; Han, H. *J Polym Sci Polym Phys* 2001, 39, 669.
22. Japanese Industrial Standard JIS Z 2801, 2000.
23. Hong, R.; Pan, T.; Qian, J.; Li, H. *Chem Eng J* 2006, 119, 71.
24. Liu, B.; Chen, L.; Zhang, M.; Yu, A. *Macromol Rapid Commun* 2002, 23, 881.
25. Emamifar, A.; Kadivar, M.; Shahedi, M.; Soleimani-Zad, S. *Food Control* 2010, 22, 408.
26. Li, X. H.; Xing, W. L.; Li, W. L.; Jiang, Y. H.; Ding, Y. L. *Food Sci Technol Int* 2010, 16, 225.